Supporting Information

Linear red/green ratiometric thermometry of Ho^{3+}/Cr^{3+} co-doped red up-conversion tungstate materials

Yan Zhao,[a] Xusheng Wang,*[,a] Rui Hu,[a,b,c] and Yanxia Li[a]

[a] Key Laboratory of Advanced Civil Engineering Materials of the Ministry of Education, Functional Materials Research Laboratory, School of Materials Science and Engineering, Tongji University, 4800 Cao'an Road, Shanghai 201804, China

[b] The Key Laboratory of Inorganic Functional Materials and Devices, Shanghai Institute of Ceramics, Chinese Academy of Sciences, Shanghai 200050, China

[c] University of Chinese Academy of Sciences, Beijing 100049, China

*Corresponding authors: Xusheng Wang (xs-wang@tongji.edu.cn)

Table S1 The characterization methods, instruments and details involved in this paper.

Structure and performance	Characterization method	Test instrument	Test detail
Crystal structure	X-ray diffraction (XRD)	X-ray diffractometer (D8 Advance, Bruker Inc., Germany)	Range: $10° \leq 2\theta \leq 70°$ Speed: 3°/min
Microstructure	Scanning electron microscopy (SEM)	(Hitachi S4800, Japan)	
Elemental analysis	Energy disperse spectroscopy (EDS)	(Quantaax 200, Bruker, Germany)	Area scan
	X-ray photoelectron spectroscopy (XPS)	(ESCALAB 250, Thermo Fisher) equipped with a focused monochromatic Al Kα X-ray beam	Range: 100 ~ 2000 nm
Optical performance	Raman spectrum	Raman spectrophotometer (LabRAM HR, Horiba Jobin Yvon, France) with a 532 nm laser	
	UV-vis absorption spectrum	UV-vis spectrophotometer (Shimadzu UV-2550, Tokyo, Japan)	Range: 100 ~ 1000 nm Speed: 300 nm/min
	UC luminescence	Fluorescence spectrophotometer (F-7000, Hitachi High-Technologies Corporation, Tokyo, Japan) with a 980 nm laser diode (HJZ980-100)	Range: 500 ~ 700 nm speed:1200 nm/min
	Temperature sensing performance	An additional heated stage controlled by a TP94 temperature controller (Linkam Scientific Instruments Ltd., Surrey, UK)	Range: -80 ~ 390 °C Heating rate: 10℃/min Interval point: 30℃/point Standing time: 5 min/point

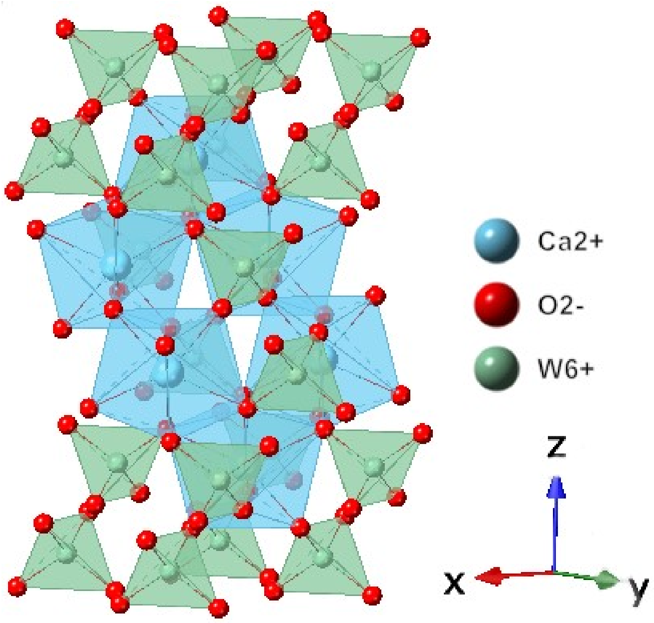

Fig. S1 Crystal structure of $CaWO_4$.

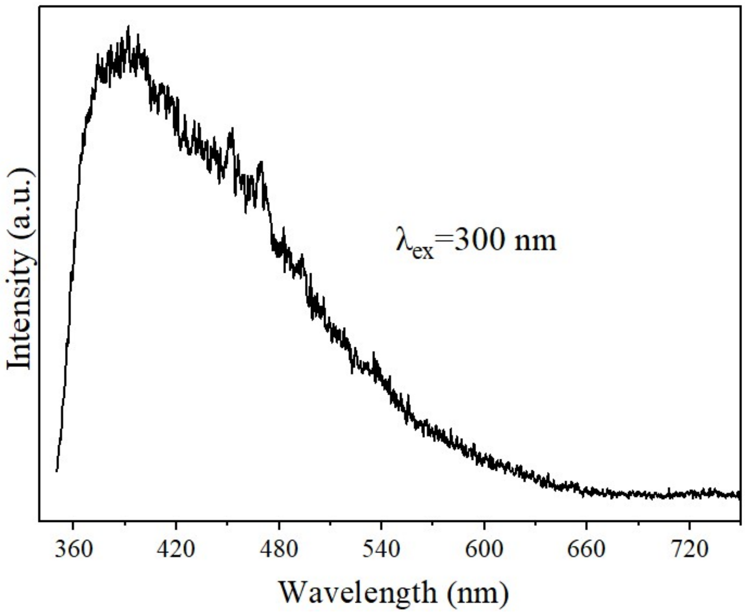

Fig. S2 Intrinsic emission spectrum of matrix $CaWO_4$.

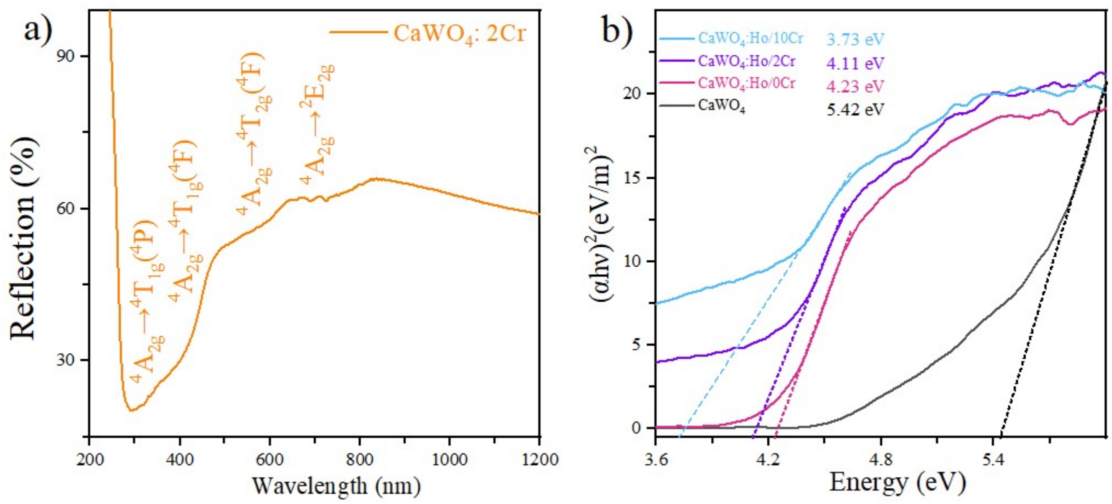

Fig. S3 a) UV-vis diffuse reflection spectrum of $CaWO_4$: 2mol%Cr phosphor. b) Transformed Kubelka-Munk spectra of $CaWO_4$ and $CaWO_4$:Ho/100xCr phosphors (x = 0.0, 0.02, and 0.1), respectively.

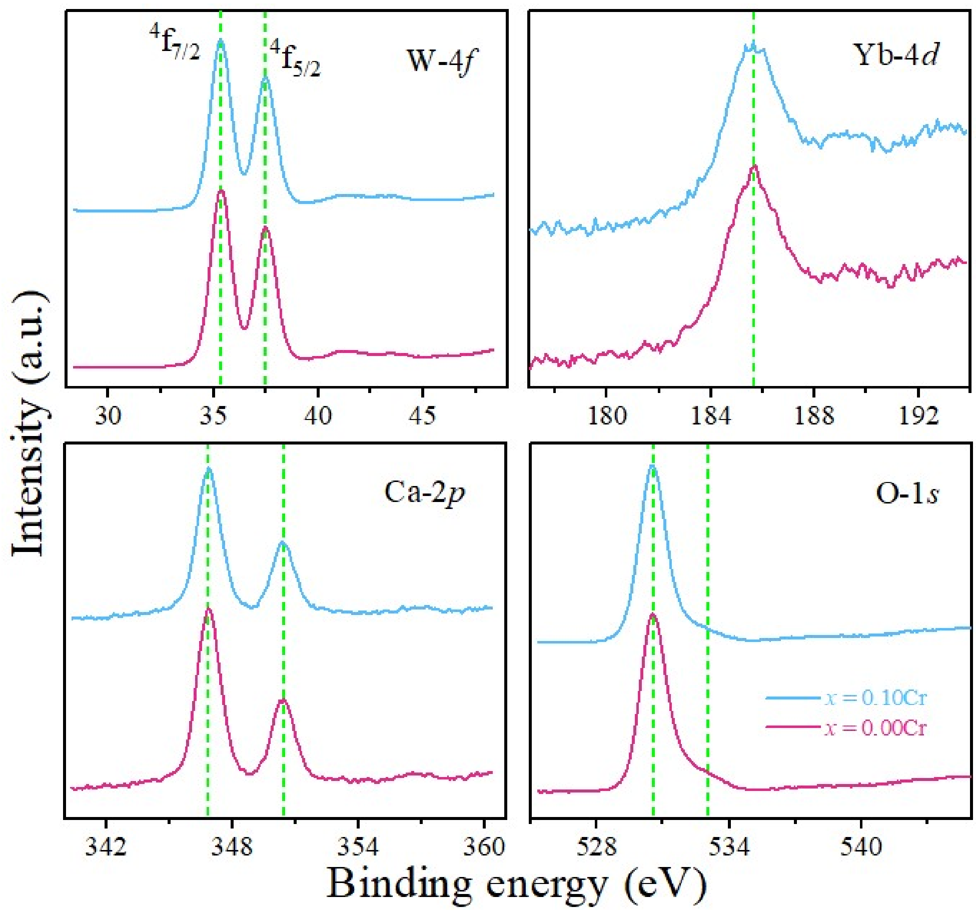

Fig. S4 High resolution XPS spectra of W 4f, Yb 4d, Ca 2p and O 1s elements in $CaWO_4$:Ho/0Cr and $CaWO_4$:Ho/10Cr sample.

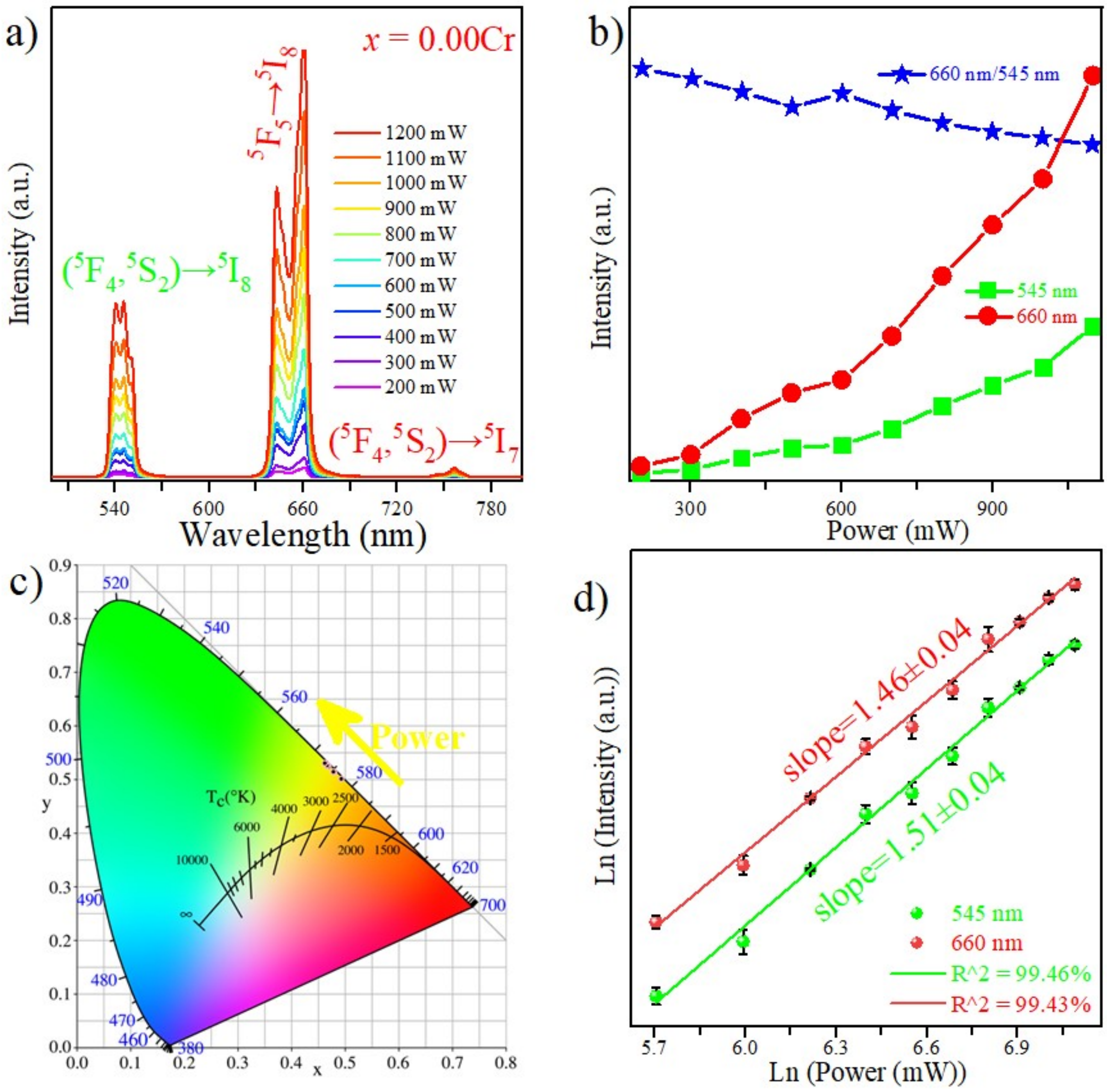

Fig. S5 UC luminescence spectra, b) green, red intensity and R/G intensity ratio, c) CIE chromaticity with different excitation power, and d) Doubles logarithmic curves of the emission intensity *versus* excitation power of $CaWO_4$:Ho/0Cr phosphor under 980 nm excitation.

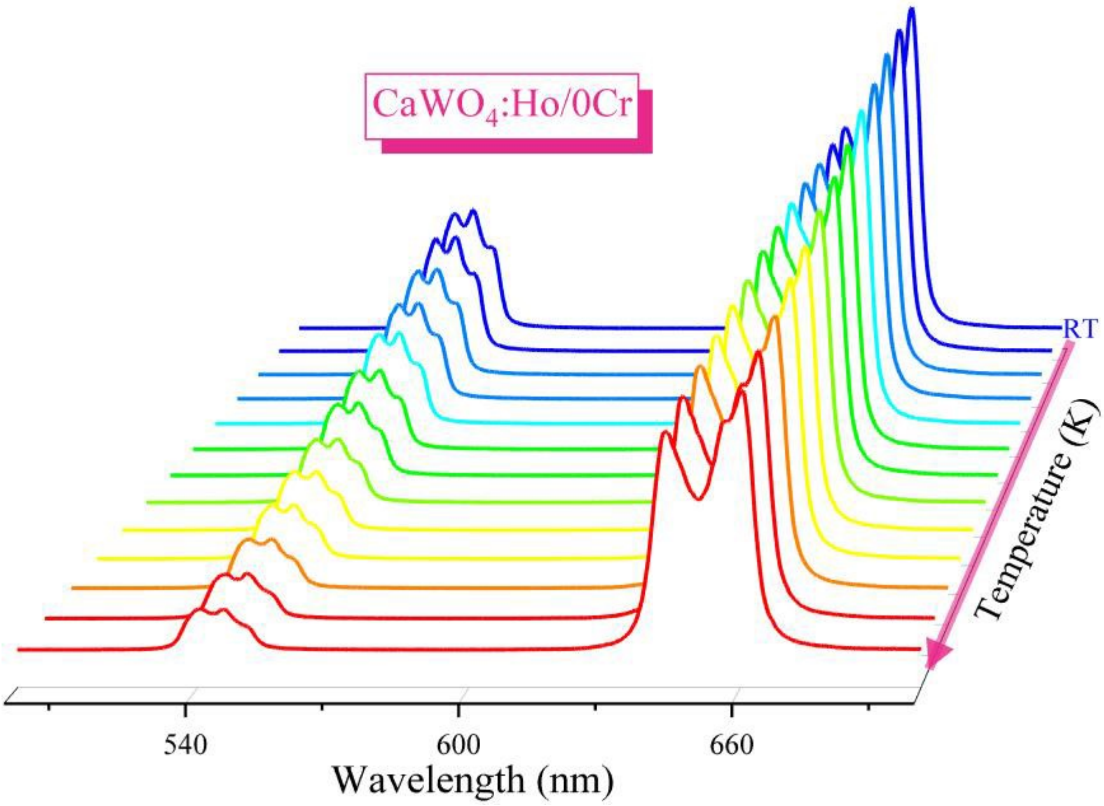

Fig. S6 UC emission spectra with a 3D model of $CaWO_4$:Ho/0Cr phosphor under 980 nm excitation over the temperature range from RT to 663 K.

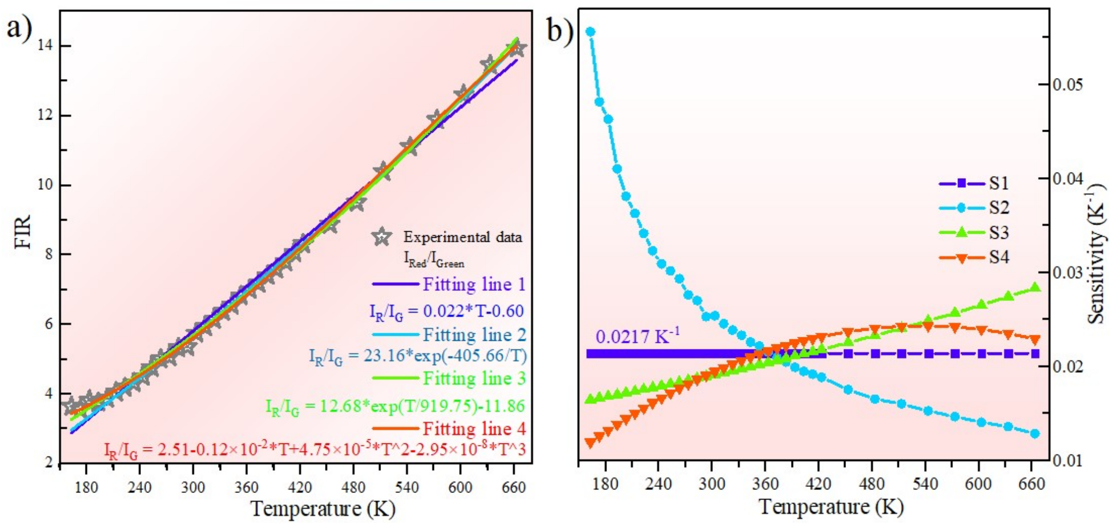

Fig. S7 a) Fitting situation of Formula 1-4 with experimental data, and b) Corresponding sensitivity values after fitting of $CaWO_4$:Ho/2Cr phosphor under 980 nm excitation over the temperature range from 163 K to 663 K.

Common LIR thermometry technology is also based on the sensitive relationship between the intensity ratio of two transition levels and temperature, independent of spectral loss and fluctuation of excitation intensity, and has high precision and resolution. Theoretically, the two transition levels must be thermally coupled; that is, the energy level difference is within the range of 200 ~ 2000 cm^{-1}. So the two Ho^{3+} transitions ($^5F_4$, $^5S_2$) → $^5I_8$ (Green) and $^5F_5$ → $^5I_8$ (Red) with the difference of ~3000 cm^{-1}, are clearly not thermally coupled. At present, the sensitivity of the non-thermally coupled R/G ratio to temperature has not been determined, and a variety of fitting formulas have been reported, including linear, exponential, etc. (Formula 1-4). For any strategy mentioned above, enhancing the sensitivity of the optical thermometer effectively has always been an important object for researchers. In order to highlight the comparability of $CaWO_4$:Ho/2Cr sample, these four strategies were verified successively. These four formulas were in good agreement with the experimental data, and the standard errors were within the acceptable range. The fitting curves of the experimental data of $CaWO_4$:Ho/2Cr sample and Formula 1-4 were shown in Fig. S7a), together with the fitted formulas. The corresponding sensitivity values were obtained by taking the derivative of the fitting formulas with respect to temperature (Fig. S7b). Comparison of specific sensitivity values was presented in Table S2. For strategy 1, although a high sensitivity of 0.0452 K^{-1} in the range of 293-453 K has been reported, linearity could not be fitted at temperatures above 453 K, and studies at low temperatures were lacking.[1] For strategy 2, the sensitivity value in this paper decreased rapidly in the temperature range 163-663 K, but it was superior to the reported literature in both high and low temperatures.[2] For strategies 3 and 4, the reported literature lacked studies at low temperature, and the sensitivity at RT was very low.[3] These results indicated that the incorporation of Cr^{3+} improved the sensitivity of the sample in a wide temperature range, and the $CaWO_4$:Ho/2Cr material has a good application potential in optical temperature sensing field.

Table S2 Comparison of sensitivity and temperature sensing regions of Ho^{3+} in different host materials under different temperature measurement strategies.

Materials	Transition	S_{max} ($\times10^{-4}$ K^{-1})	S_{min} ($\times10^{-4}$ K^{-1})	Fitting formula	Ref.
$CaWO_4:Ho^{3+}/Yb^{3+}/Li^{+}/Cr^{3+}$	$^5F_5/(^5F_4,^5S_2)\rightarrow{}^5I_8$	233 (RT-663 K)	164 (163 K-RT)	Formula 1	This
	$^5F_5/(^5F_4,^5S_2)\rightarrow{}^5I_8$	217 (163-663 K)		Formula 1	work
	$^5F_5/(^5F_4,^5S_2)\rightarrow{}^5I_8$	556 (163 K)	129 (663 K)	Formula 2	
	$^5F_5/(^5F_4,^5S_2)\rightarrow{}^5I_8$	284 (663 K)	165 (163 K)	Formula 3	
	$^5F_5/(^5F_4,^5S_2)\rightarrow{}^5I_8$	243 (543 K)	120 (163 K)	Formula 4	
$KLu(WO_4)_2:0.01Ho^{3+}/0.1Yb^{3+}$	$^5F_5/(^5F_4,^5S_2)\rightarrow{}^5I_8$	67 (297-673 K)		Formula 1	4
$Ba_2Gd_2Si_4O_{13}:Ho^{3+}/Yb^{3+}$	$^5F_5/(^5F_4,^5S_2)\rightarrow{}^5I_8$	452 (293-453 K)		Formula 1	1
$Y_{1.68}WO_6:0.02Ho^{3+}/0.3Yb^{3+}$	$^5F_5/(^5F_4,^5S_2)\rightarrow{}^5I_8$	110 (293-533 K)		Formula 1	5
$Sc_2Mo_3O_{12}:Ho^{3+}/Yb^{3+}$	$^5F_5/(^5F_4,^5S_2)\rightarrow{}^5I_8$	275 (545 K)	109 (303 K)	Formula 2	2
$BaTiO_3$-$0.05(Na_{0.5}Ho_{0.5})TiO_3$	$^5F_4/^5S_2\rightarrow{}^5I_8$	63 (600 K)		Formula 2	6
$(K_{0.47}Na_{0.47}Li_{0.06})(Nb_{0.94}Bi_{0.06})O_3:Ho^{3+}$	$^5F_4/^5S_2\rightarrow{}^5I_8$	75 (430 K)	57 (300 K)	Formula 2	7
$0.9(K_{0.5}Na_{0.5})NbO_3$-$0.1SrTiO_3:0.01Ho^{3+}$	$^5F_4/^5S_2\rightarrow{}^5I_8$	89 (540 K)	57 (293 K)	Formula 2	8
$Bi_{0.5}Na_{0.5}TiO_3:0.5at\%Ho^{3+}$	$^5F_4/^5S_2\rightarrow{}^5I_8$	21.1 (377 K)	0.9 (167 K)	Formula 2	9
$Ca_2Gd_8(SiO_4)_6O_2:3\%Ho^{3+}/10\%Yb^{3+}$	$^5F_5/(^5F_4,^5S_2)\rightarrow{}^5I_8$	1110 (533 K)	100 (350 K)	Formula 3	10
$NaLaMgWO_6:Ho^{3+}/Yb^{3+}$	$^5F_5/(^5F_4,^5S_2)\rightarrow{}^5I_8$	89 (548 K)	20 (298 K)	Formula 3	3
$Ba_9Y_{1.52}Si_6O_{24}:0.08Ho^{3+}/0.4Yb^{3+}$	$(^5F_4,^5S_2)/^5F_5\rightarrow{}^5I_8$	580 (293 K)	50 (553 K)	Formula 3	11
$Gd_6O_5F_8:0.3\%Ho^{3+}/5\%Yb^{3+}/7\%Li^{+}$	$(^5F_4,^5S_2)/^5F_5\rightarrow{}^5I_8$			Formula 3	12
$NaGdF_4:Ho^{3+}/Yb^{3+}$	$^5F_5/(^5F_4,^5S_2)\rightarrow{}^5I_8$	1700 (523 K)	100 (303 K)	Formula 4	13

References

1. J. Zhang, X. Jiang and Z. Hua, *Ind. Eng. Chem. Res.*, 2018, **57**, 7507-7515.
2. H. Zou, B. Chen, Y. Hu, Q. Zhang, X. Wang and F. Wang, *J. Phys. Chem. Lett.*, 2020, **11**, 3020-3024.
3. J. Zhang and C. Jin, *J. Alloys Compd.*, 2019, **783**, 84-94.
4. O. A. Savchuk, J. J. Carvajal, M. C. Pujol, E. W. Barrera, J. Massons, M. Aguilo and F. Diaz, *J. Phys. Chem. C*, 2015, **119**, 18546-18558.
5. J. Zhang, B. Ji, G. Chen and Z. Hua, *Inorg. Chem.*, 2018, **57**, 5038-5047.
6. J. Li, X. Chai, X. Wang, C. N. Xu, Y. Gu, H. Zhao and X. Yao, *Dalton Trans*, 2016, **45**, 11733-11741.
7. X. Wu, J. Lin, P. Chen, C. Liu, M. Lin, C. Lin, L. Luo and X. Zheng, *J. Am. Ceram. Soc.*, 2019, **102**, 1249-1258.
8. J. Lin, Q. Lu, J. Xu, X. Wu, C. Lin, T. Lin, C. Chen and L. Luo, *J. Am. Ceram. Soc.*, 2019, **102**, 4710-4720.
9. Y. Wang, Y. Wang, C. Ma, Z. Feng, C. Zuo, W. Ye, C. Zhao, Y. Li, Z. Wen, Z. Cao, Z. Cao, X. Shen, C. Wang, Y. Li, X. Yuan and Y. Cao, *J. Mater. Chem. C*, 2021, **9**, 1353-1361.
10. J. Zhang, G. Chen, Z. Zhai, H. Chen and Y. Zhang, *J. Alloys Compd.*, 2019, **771**, 838-846.
11. J. Zhang, X. Li and G. Chen, *Mater. Chem. Phys.*, 2018, **206**, 40-47.
12. S. Du, D. Wang, Q. Qiang, X. Ma, Z. Tang and Y. Wang, *J. Mater. Chem. C*, 2016, **4**, 7148-7155.
13. Q. Qiang and Y. Wang, *New J. Chem.*, 2019, **43**, 5011-5019.